Inorganic Chemistry

Article

pubs.acs.org/IC

Effects of the Alkali-Metal Cation Size on Molecular and Extended Structures: Formation of Coordination Polymers and Hybrid Materials in the Homologous Series [(4-Et-C_6H_4OM)·$(diox)_n$], M = Li, Na, K, Rb, Cs

Jeffrey A. Bertke, Allen G. Oliver, and Kenneth W. Henderson*

Department of Chemistry and Biochemistry, University of Notre Dame, Notre Dame, Indiana 46556, United States

Supporting Information

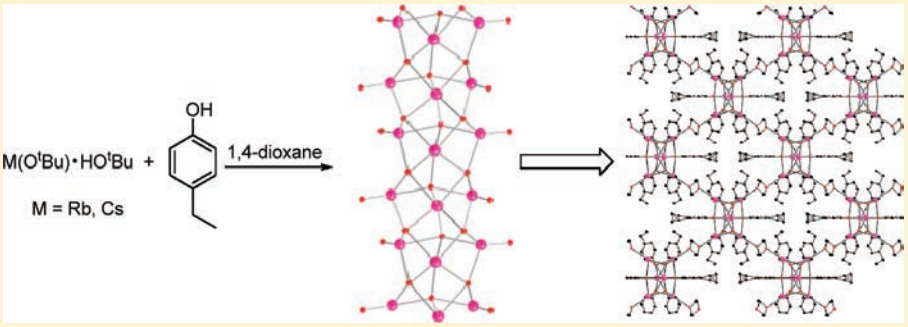

ABSTRACT: The complete series of group 1 metal 4-ethylphenoxide (4-Et-$C_6H_4O^-$) networks have been synthesized using 1,4-dioxane (diox) as a neutral linker. $[\{(4\text{-Et-}C_6H_4OLi)_4\cdot(diox)_{2.5}\}\cdot diox]_\infty$ (**1**) and $[\{(4\text{-Et-}C_6H_4ONa)_6\cdot(diox)_3\}_\infty]$ (**2**) form 2D and 3D networks, respectively, composed of discrete aggregates linked by diox. Compound **1** forms a hexagonal layered structure with Li_4O_4 cubanes acting as nodes, whereas compound **2** forms a primitive cubic network (**pcu**) with Na_6O_6 hexameric nodes. $[\{(4\text{-Et-}C_6H_4OK)_3\cdot diox\}_\infty]$ (**3**), $[\{(4\text{-Et-}C_6H_4ORb)_2\cdot(diox)_{0.5}\}_\infty]$ (**4**), and $[\{(4\text{-Et-}C_6H_4OCs)_2\cdot(diox)_{0.5}\}_\infty]$ (**5**) are composed of isostructural 1D inorganic rods that are linked through diox to form **pcu**-type networks. Compound **5** is the first example of a network built from cesium inorganic rods.

INTRODUCTION

The synthesis and characterization of metal−organic frameworks (MOFs) is currently an area of intense interest.[1−5] One common method for synthesizing MOFs is the building-block approach, in which a preassembled metal aggregate is used as a secondary building unit (SBU).[4−6] The SBUs are then connected through a multitopic organic linker to build the extended structure. A less common approach is the use of one-dimensional (1D) inorganic rods as building units. An inorganic rod is simply a 1D polymer built entirely from M−X (X = N, O, S, etc.) interactions. They differ from molecular SBUs in that no organic linker is necessary to build the polymer. Similar to molecular SBUs, these inorganic rods can be connected through organic linkers to form hybrid organic−inorganic materials.[7−11] The hybrid systems have the potential to display desirable properties such as increased thermal and chemical stabilities in comparison to other coordination polymers. Also, if structural patterns begin to emerge as more of these materials are characterized, it will lead to an increased ability to design such MOFs a priori. To date, very few examples of alkali-metal aryloxide rods have been reported.[10,12,13]

Our group has focused on the use of alkali-metal aggregates as SBUs in constructing MOFs. The well-known aggregation states of organo-alkali-metal complexes[14−18] lend themselves quite well to use as SBUs. Most of this chemistry has focused on the lighter alkali metals, lithium and sodium.[19−26] While some work has been done with the heavier metals, potassium, rubidium, and cesium, their chemistry in this area is largely unexplored.[10,27−29] In part, this is a consequence of the more advanced understanding of the coordination chemistry of organolithium and -sodium complexes. In addition, the increased reactivity of the heavier alkali metals makes their preparation and handling more challenging. Nevertheless, the limited work completed on heavy-alkali-metal aryloxide complexes has produced some very interesting results. Two of the five reported 7-connected uninodal networks[30−32] are built from potassium and rubidium,[27] and the first of three reported 9-connected uninodal networks[33,34] is a rubidium framework.[27] In hopes of building on these interesting results and expanding on our understanding of alkali-metal supramolecular chemistry, the alkali metal/4-Et-$C_6H_4O^-$/1,4-dioxane system was studied in a systematic manner. The lithium and sodium analogues have previously been communicated and were found to form tetrameric and hexameric SBUs,

Received: October 5, 2011
Published: December 23, 2011

dx.doi.org/10.1021/ic202158m | *Inorg. Chem.* 2012, 51, 1020−1027

respectively.[22,23] This increase in aggregation state led us to focus on the effect of increasing the ionic radius of the metal center on both the molecular and supramolecular structures. Here we report the synthesis and characterization of the complete group 1 series with the 4-Et-$C_6H_4O^-$/1,4-dioxane system.

This series of networks represents only the second homologous series of group 1 nonfunctionalized aryloxide compounds reported in the literature.[13] The first homologous series is the solvent-free alkali-metal phenoxide system metal/$C_6H_5O^-$.[13] The solid-state structures of these compounds were determined via Rietveld refinement of powder X-ray diffraction data. The crystallinity of the lithium compound was too poor to allow for structure solution; the other four homologues form 1D inorganic rods. These rods will be discussed later.

There have also been several homologous nitro-functionalized aryloxide series reported.[35−40] Nonaryloxide examples of homologous alkali-metal complexes have been characterized, for example, the hexamethyldisilazide[41−44] and *tert*-butoxide[45,46] series.

EXPERIMENTAL SECTION

General Procedures. All experimental manipulations were performed under a dry nitrogen atmosphere in flame-dried glassware using standard Schlenk techniques. 1,4-Dioxane was distilled from sodium benzophenone and stored over 4 Å molecular sieves prior to use. Hexane was dried by passage through columns of a copper-based catalyst and alumina (Innovative Technology). BuLi was purchased from Aldrich as a 1.6 M solution in hexane and was standardized by titration against salicylaldehyde phenylhydrazone directly before use. NaH was purchased from Aldrich and used as received. K[$N(SiMe_3)_2$] was purchased from Fluka and used without further purification. Rb(O^tBu) and Cs(O^tBu) were synthesized via literature methods.[46] 4-Ethylphenol was purchased from Lancaster and dried by recrystallization from hexane prior to use. NMR spectra were obtained on a Varian Unity Plus 300 MHz instrument. Nonintegral values for 1,4-dioxane are due to partial removal under vacuum upon isolation. ^1H and ^{13}C NMR spectra were referenced with respect to the residual solvent signal. Fourier transform infrared (FTIR) spectra were obtained on a Nicolet Nexus 670 FTIR spectrometer under a stream of flowing nitrogen.

X-ray Crystallography. Single crystals were examined under Infineum V8512 oil. The datum crystal was affixed to a Mitegen mounting loop and transferred to the 100 K nitrogen stream of a Bruker APEX diffractometer equipped with an Oxford Cryosystems 700 series low-temperature apparatus. Cell parameters were determined using reflections harvested from three sets of 12 0.5° φ scans. The orientation matrix derived from this was transferred to COSMO to determine the optimum data collection strategy requiring a minimum of 4-fold redundancy. Cell parameters were refined using reflections harvested from data collection with $I \geq 10\sigma(I)$. All data were corrected for Lorentz and polarization effects, and runs were scaled using *SADABS*. The structures were solved and refined using *SHELXTL*. Structure solution was by direct methods. Non-hydrogen atoms not present in the direct methods solution were located by successive cycles of the full-matrix least-squares refinement on F^2. All non-hydrogen atoms were refined with parameters for anisotropic thermal motion. Hydrogen atoms were placed at calculated geometries and allowed to ride on the position of the parent atom. Hydrogen thermal parameters were set to 1.2 times the equivalent isotropic U of the parent atom.

Synthesis of [{(4-Et-$C_6H_4OLi)_4$·(dioxo)$_{2.5}$}·dioxo]$_\infty$ (1).[22] BuLi (5 mmol, 3.2 mL) was added to a stirred solution of 4-ethylphenol (5 mmol, 621 mg) in 1,4-dioxane (5 mL). Upon the addition of hexane (12 mL), a white precipitate formed, which dissolved upon heating. Crystalline material was obtained by slowly cooling the resulting solution in a hot water bath. Yield: 650 mg, 72.9%. ^1H NMR (300 MHz, DMSO-d_6, 25 °C): δ 1.13 (t, $^3J_{HH}$ = 7.5 Hz, 3H, CH_3, Et), 2.44 (q, $^3J_{HH}$ = 7.8 Hz, 2H, CH_2, Et), 3.59 (s, 4.6H, OCH_2, dioxane), 6.50 (d, $^3J_{HH}$ = 8.1 Hz, 2H,*o*-H, Ph), 6.79 (d, $^3J_{HH}$ = 8.1 Hz, 2H, *m*-H, Ph). $^{13}C\{^1H\}$ NMR (75 MHz, DMSO-d_6, 25 °C): δ 16.86 (CH_3, Et), 27.70 (CH_2, Et), 66.46 (OCH_2, dioxane), 119.44 (*o*-C, Ph), 126.71 (*p*-C, Ph), 127.70 (*m*-C, Ph), 166.24 (*i*-C, Ph).

Synthesis of [{(4-Et-$C_6H_4ONa)_6$·(dioxo)$_3$}$_\infty$] (2).[23] 4-Ethylphenol (5 mmol, 610 mg) was added to a stirred suspension of sodium hydride (5 mmol, 120 mg) in 1,4-dioxane (5 mL) to give a white precipitate. Complete dissolution was achieved upon heating. X-ray-quality crystals were precipitated upon the slow evaporation of the solvent within a glovebox. Yield: 660 mg, 78.1%. ^1H NMR (300 MHz, DMSO-d_6, 25 °C): δ 1.07 (3H, t, $^3J_{HH}$ = 7.5 Hz, CH_3, Et), 2.34 (2H, q, $^3J_{HH}$ = 7.5 Hz, CH_2, Et), 3.57 (2.2 H, s, OCH_2, dioxane), 6.14 (2 H, d, $^3J_{HH}$ = 8.4 Hz, *m*-H, Ph), 6.54 (2H, d, $^3J_{HH}$ = 8.1 Hz, *o*-H, Ph). $^{13}C\{^1H\}$ NMR (75 MHz, DMSO-d_6, 25 °C): δ 18.82 (CH_3, Et), 27.60 (CH_2, Et), 66.39 (OCH_2, dioxane), 118.44 (*o*-C, Ph), 122.87 (*m*-C, Ph), 127.94 (*p*-C, Ph), 168.87 (*i*-C, Ph).

Synthesis of [{(4-Et-$C_6H_4OK)_3$·dioxo}$_\infty$] (3). K[$N(SiMe_3)_2$] (3 mmol, 600 mg) was added to a stirred solution of 4-ethylphenol (3 mmol, 366 mg) in 1,4-dioxane (10 mL) to give a white precipitate. An additional 15 mL of 1,4-dioxane was added, and complete dissolution was achieved upon heating. X-ray-quality crystals were obtained by the slow cooling of the solution in a hot water bath. Crystalline yield: 490 mg, 29%. Sample decomposed at 198 °C. ^1H NMR (300 MHz, pyridine-d_5, 25 °C): δ 1.23 (3H, t, $^3J_{HH}$ = 7.5 Hz, CH_3, Et), 2.58 (2H, q, $^3J_{HH}$ = 7.1 Hz, CH_2, Et), 3.63 (4H, s, OCH_2, dioxane), 6.87 (2H, d, $^3J_{HH}$ = 7.3 Hz, *o*-H, Ph), 7.04 (2H, d, $^3J_{HH}$ = 8.1 Hz, *m*-H, Ph). $^{13}C\{^1H\}$ NMR (75 MHz, pyridine-d_5, 25 °C): δ 17.74 (CH_3, Et), 29.07 (CH_2, Et), 67.64 (OCH_2, dioxane), 119.56 (*o*-C, Ph), 124.99 (*m*-C, Ph), 130.15 (*p*-C, Ph), 171.25 (*i*-C, PH). FTIR (Nujol mull, cm^{-1}): 1600 (w), 1498 (m), 1322 (m), 1310 (m), 1165 (w), 1113 (w), 841 (w), 720 (w).

Synthesis of [{(4-Et-$C_6H_4ORb)_2$·(dioxo)$_{0.5}$}$_\infty$] (4). [Rb(O^tBu)·HO^tBu] (2 mmol, 465 mg) was added to a stirred solution of 4-ethylphenol (2 mmol, 244 mg) in 1,4-dioxane (10 mL) to give a white precipitate. An additional 10 mL of 1,4-dioxane was added, the mixture was heated, and *N*,*N*-dimethylformamide (1.5 mL) was added dropwise until complete dissolution was achieved. X-ray-quality crystals were obtained by the slow cooling of the solution in a hot water bath. Crystalline yield: 281 mg, 31%. Sample decomposed at 198 °C. ^1H NMR (300 MHz, pyridine-d_5, 25 °C): δ 1.25 (3H, t, $^3J_{HH}$ = 7.3 Hz, CH_3, Et), 2.59 (2H, q, $^3J_{HH}$ = 7.5 Hz, CH_2, Et), 3.63 (2H, s, OCH_2, dioxane), 6.84 (2H, d, $^3J_{HH}$ = 8.3 Hz, *o*-H, Ph), 7.06 (2H, d, $^3J_{HH}$ = 8.3 Hz, *m*-H, Ph). $^{13}C\{^1H\}$ NMR (75 MHz, pyridine-d_5, 25 °C): δ 17.63 (CH_3, Et), 29.06 (CH_2, Et), 67.64 (OCH_2, dioxane), 119.70 (*o*-C, Ph), 125.22 (*m*-C, Ph), 130.18 (*p*-C, Ph), 170.57 (*i*-C, PH). FTIR (Nujol mull, cm^{-1}): 1598 (w), 1498 (m), 1313 (m), 1164 (w), 1115 (w), 839 (w), 720 (w).

Synthesis of [{(4-Et-$C_6H_4OCs)_2$·(dioxo)$_{0.5}$}$_\infty$] (5). [Cs(O^tBu)·HO^tBu] (2 mmol, 560 mg) was added to a stirred solution of 4-ethylphenol (2 mmol, 244 mg) in 1,4-dioxane (10 mL) to give a white precipitate. Complete dissolution was achieved upon heating. X-ray-quality crystals were obtained by the slow cooling of the solution in a hot water bath. Crystalline yield: 198 mg, 18%. Mp: 188 °C. ^1H NMR (300 MHz, pyridine-d_5, 25 °C): δ 1.25 (3H, t, $^3J_{HH}$ = 7.5 Hz, CH_3, Et), 2.59 (2H, q, $^3J_{HH}$ = 7.5 Hz, CH_2, Et), 3.63 (1.5H, s, OCH_2, dioxane), 6.84 (2H, d, $^3J_{HH}$ = 8.3 Hz, *o*-H, Ph), 7.10 (2H, d, $^3J_{HH}$ = 8.5 Hz, *m*-H, Ph). $^{13}C\{^1H\}$ NMR (75 MHz, pyridine-d_5, 25 °C): δ 17.56 (CH_3, Et), 29.03 (CH_2, Et), 67.64 (OCH_2, dioxane), 114.74 (*o*-C, Ph), 120.04 (*m*-C, Ph), 130.31 (*p*-C, Ph), 170.01 (*i*-C, PH). FTIR (Nujol mull, cm^{-1}): 1598 (m), 1496 (s), 1313 (m), 1164 (m), 1117 (w), 871 (w), 838 (m), 721 (w).

RESULTS AND DISCUSSION

The synthesis of **1**−**5** involved the reaction of 4-ethylphenol with the appropriate organometallic reagent in a 1,4-dioxane solution (eqs 1−5). Compounds **1**−**5** can be divided into two groups: those that form discrete SBUs and those that form inorganic rods. The previously reported complexes **1** and **2** are

dx.doi.org/10.1021/ic202158m | *Inorg. Chem.* 2012, 51, 1020−1027

constructed of molecular aggregates that are linked to form networks. Compounds **3**–**5**, however, are constructed of 1D inorganic rods that are linked to form networks.

$$4^{n}\mathrm{BuLi} + 4(4\text{-Et-}C_6H_4OH) \xrightarrow{1,4\text{-dioxane}} [\{(4\text{-Et-}C_6H_4OLi)_4\cdot(\mathrm{diox})_{2.5}\}\cdot\mathrm{diox}]_\infty \quad (1)$$

$$6\mathrm{NaH} + 6(4\text{-Et-}C_6H_4OH) \xrightarrow{1,4\text{-dioxane}} [(4\text{-Et-}C_6H_4ONa)_6\cdot(\mathrm{diox})_3]_\infty \quad (2)$$

$$3\mathrm{K[N(SiMe_3)_2]} + 3(4\text{-Et-}C_6H_4OH) \xrightarrow{1,4\text{-dioxane}} [(4\text{-Et-}C_6H_4OK)_3\cdot(\mathrm{diox})]_\infty \quad (3)$$

$$2\mathrm{Rb(O^tBu)\cdot HO^tBu} + 2(4\text{-Et-}C_6H_4OH) \xrightarrow{1,4\text{-dioxane}} [(4\text{-Et-}C_6H_4ORb)_2\cdot(\mathrm{diox})_{0.5}]_\infty \quad (4)$$

$$2\mathrm{Cs(O^tBu)\cdot HO^tBu} + 2(4\text{-Et-}C_6H_4OH) \xrightarrow{1,4\text{-dioxane}} [(4\text{-Et-}C_6H_4OCs)_2\cdot(\mathrm{diox})_{0.5}]_\infty \quad (5)$$

Tables 1 and 2 contain the data collection parameters for **1**–**5**. The molecular structure of **1** is composed of a tetrameric $[(4\text{-Et-}C_6H_4O)Li]_4$ cubane in which each metal center is solvated by 1,4-dioxane (Figure 1). Aggregates are very common in organo-

Table 1. Crystallographic Data for Compounds 1 and 2

	1	2
formula	$C_{92}H_{128}Li_8O_{22}$	$C_{30}H_{39}Na_3O_6$
fw	1641.46	564.58
wavelength/Å	0.710 73	0.710 73
cryst syst	triclinic	monoclinic
space group	$P\bar{1}$	$P2(1)/c$
a/Å	14.3172(3)	10.3777(1)
b/Å	15.2696(3)	16.5849(2)
c/Å	24.5935(6)	17.9530(2)
α/deg	74.194(1)	
β/deg	84.994(1)	95.596(1)
γ/deg	62.507(1)	
V/Å^3	4584.39(17)	3075.22(6)
Z	2	4
d_{calc}/ g cm^{-3}	1.189	1.219
size/mm	0.34 × 0.30 × 0.26	0.45 × 0.36 × 0.31
$\mu(\lambda)$/mm^{-1}	0.082	0.119
max/min transmn	0.9787/0.9726	0.9641/0.8866
reflns collected	91 923	43 096
indep reflns	22 586	10 149
param refined	1107	352
R(int)	0.0389	0.0245
R1, wR2 [$I > 2\sigma(I)$]	0.0575, 0.1584	0.0365, 0.1032
R1, wR2 (all data)	0.0810, 0.1782	0.0487, 0.1084
GOF on F^2	1.044	1.096
largest peak, hole/e Å^{-3}	0.982, −0.450	0.447, −0.184

Table 2. Crystallographic Data for Compounds 3–5

	3	4	5
formula	$C_{28}H_{35}K_3O_5$	$C_{29}H_{30}O_5Rb_3$	$C_{28}H_{30}Cs_3O_5$
fw	568.86	714.94	845.25
wavelength/ Å	1.541 78	1.541 78	1.541 78
cryst syst	monoclinic	orthorhombic	orthorhombic
space group	$P2(1)/c$	$Pnma$	$Pnma$
a/Å	19.2016(12)	7.4579(3)	7.8905(3)
b/Å	20.4584(12)	19.2403(6)	19.0010(7)
c/Å	7.2704(5)	21.0434(6)	21.1957(9)
α/deg			
β/deg	90.113(4)		
γ/deg			
V/Å^3	2856.1(3)	3019.56(18)	3177.8(2)
Z	4	4	4
d_{calc}/g cm^{-3}	1.323	1.573	1.767
size/mm	0.25 × 0.12 × 0.05	0.28 × 0.25 × 0.11	0.31 × 0.20 × 0.08
$\mu(\lambda)$/mm^{-1}	4.518	6.431	26.944
max/min transmn	0.8056/0.3921	0.5381/0.2661	0.2218/0.0438
reflns collected	24 003	13 355	15 495
indep reflns	5193	2721	3010
param refined	328	182	185
R(int)	0.0758	0.0342	0.0689
R1, wR2 [$I > 2\sigma(I)$]	0.0659, 0.1238	0.0590, 0.2025	0.0442, 0.1171
R1, wR2 (all data)	0.0956, 0.1380	0.0642, 0.2065	0.0603, 0.1298
GOF on F^2	1.053	1.656	0.906
largest peak, hole/e Å^{-3}	0.541, −0.635	1.131, −2.016	1.999, −0.903

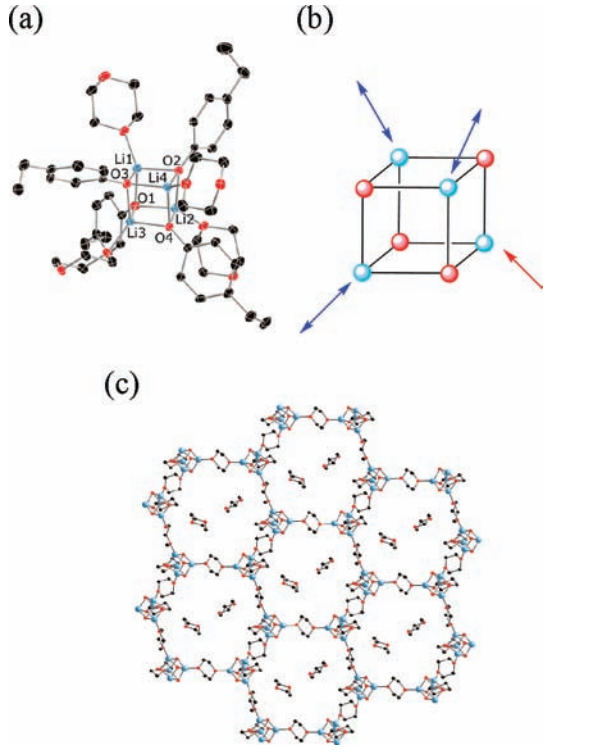

Figure 1. (a) Thermal ellipsoid plot of the tetrameric SBU of **1**. (b) SBU showing the three points of network extension (blue arrows) and the one terminally solvating 1,4-dioxane (red arrow). (c) Portion of the extended 2D structure, a (6,3) network, with two dioxane solvent molecules encapsulated in each pore. Carbon atoms of the aryl groups and all hydrogen atoms have been removed for clarity.

lithium chemistry in order to saturate the coordination sphere of the lithium atoms.[47,48] The aggregation state typically depends on the steric bulk of the anion and any solvent present, as well as electronic factors. Tetrameric lithium cubanes are a well-known structural motif in which each lithium is coordinated to three bridging anions and one solvating Lewis base.[47,48] The Li–O_{Ar} bond distances in **1** are typical of Li_4O_4 cubanes ranging from 1.90

dx.doi.org/10.1021/ic202158m | Inorg. Chem. 2012, 51, 1020–1027

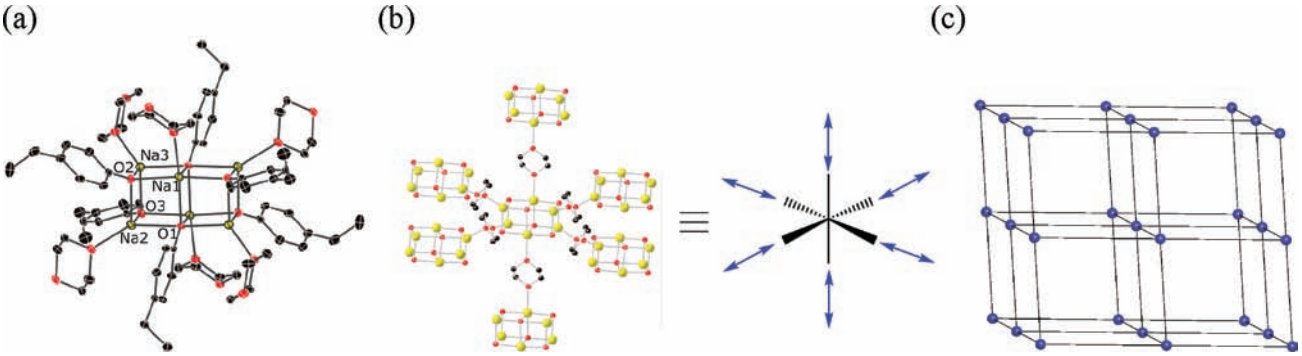

Figure 2. (a) Thermal ellipsoid plot of the hexameric SBU of **2** showing all bridging 1,4-dioxanes. (b) Portion of the extended structure of **2** showing the octahedral geometry of the SBUs. (c) Simplified view of the extended structure of **2** showing its primitive cubic (**pcu**) topology (blue balls represent Na_6O_6 clusters, and gray sticks represent bridging 1,4-dioxane).

to 1.99 Å. Comparatively, the related simple phenoxide compound $[(C_6H_5OLi)_4(diox)_3]$ has Li−O_{Ar} distances ranging from 1.92 to 1.96 Å, while the sterically more bulky compounds $[\{(C_{10}H_7OLi)_4(diox)_2\}\cdot(diox)_3]$ and $[\{(2,4,6\text{-}Me_3\text{-}C_6H_2OLi)_4(diox)_2\}\cdot(diox)_3]$ have Li−O_{Ar} distances ranging from 1.94 to 1.95 Å and from 1.98 to 2.00 Å, respectively.[22,26] Hence, these complexes all display a narrow range of cation−anion contact distances.

Tetrasolvated cubanes, such as in **1**, are good candidates for use as SBUs in building MOFs. Potentially, the cubane could act as a tetrahedral node, thus most likely building a three-dimensional (3D) diamondoid network. This is the case for $[\{(C_{10}H_7OLi)_4(diox)_2\}\cdot(diox)_3]$[22] and $[\{(2,4,6\text{-}Me_3\text{-}C_6H_2OLi)_4(diox)_2\}\cdot(diox)_3]$.[26] However, only three of the solvating 1,4-dioxanes in **1** act as linear linkers, while the fourth terminally solvates a single metal center. Consequently, the extended structure is a two-dimensional (2D) (6,3) network in which each SBU effectively acts as a trigonal node to form hexagonal sheets, as shown in Figure 1c. We have previously outlined that upon close examination of the extended structure that the 4-Et-$C_6H_4O^-$ anions are not large enough to efficiently fill the large void volume that would be present in a 3D diamondoid lattice.[22] This leads to the formation of 2D sheets that interdigitate to efficiently fill space. Also, there are two 1,4-dioxane molecules encapsulated inside the hexagonal pore, which is capped on both the top and bottom by the aryl groups. The hexameric macrocycles adopt a chair conformation, with a cross-sectional diameter of ≈17−19 Å.[22] There is one other example, of a tetrameric lithium cubane acting as an SBU for a 2D (6,3) network, namely, $[\{(Me_2NC_2H_4OLi)(2,4,6\text{-}Me_3\text{-}C_6H_2OLi)_3\cdot(diox)_{1.5}\}\cdot{}^1/_2(C_6H_{14})]$[26] This material was designed as a 2D network by incorporating a chelating anion, *N*,*N*-dimethylethanolamine, into the cubane to occupy one of the four potential points of network extension. Thus, one lithium center in the tetramer is chelated and cannot bridge to another SBU while the other three lithium metal centers are linked to neighboring SBUs via bridging 1,4-dioxane molecules. The resulting 2D sheets align to form channels that are filled with disordered hexane.

The molecular structure of **2** is composed of a hexameric $[(4\text{-}Et\text{-}C_6H_4O)Na]_6$ unit that can be described as a triple stack of dimers or two face-sharing cubanes in which each metal center is solvated by a 1,4-dioxane molecule (Figure 2). Hexameric sodium aggregates are also well-known structural motifs.[23,49] The aggregation is similar to lithium tetramers in that it aids in saturating the coordination sphere of the sodium atoms. However, because sodium has a larger ionic radius than lithium, the metals can accommodate a larger number of ligands, e.g., the five-coordinate metal centers in the center of the hexameric aggregates in **2**. The Na−O_{Ar} distances in **2** are within the expected range. The bond distances range from 2.24 to 2.44 Å for the four-coordinate metals and from 2.33 to 2.40 Å for the five-coordinate metals. These are comparable to similar complexes $[(C_6H_5ONa)_6(THF)_6]$ and $[\{(4\text{-}F\text{-}C_6H_4ONa)_6(diox)_3\}\cdot diox]$, with distances ranging between 2.23−2.36 and 2.23−2.48 Å for four-coordinate metals and between 2.36−2.40 and 2.32−2.43 Å for five-coordinate metals, respectively.[23,49]

The sodium triple stack of the dimers motif has been reported several times in both MOFs and molecular species with anions ranging from hydrazides,[50] oxides[23,49,51,52] and thiolates.[53] In **2**, each metal center is solvated by a 1,4-dioxane that bridges to another SBU. The extended structure is a 3D network with a primitive cubic (**pcu**) topology, in which each SBU acts as an octahedral node. Previously, $[\{(4\text{-}F\text{-}C_6H_4ONa)_6(diox)_3\}\cdot diox]$ was characterized as containing a sodium triple stack of dimers acting as octahedral SBUs in building a **pcu** MOF.[23] Upon examination of the extended structure of **2**, it becomes apparent that the cubic

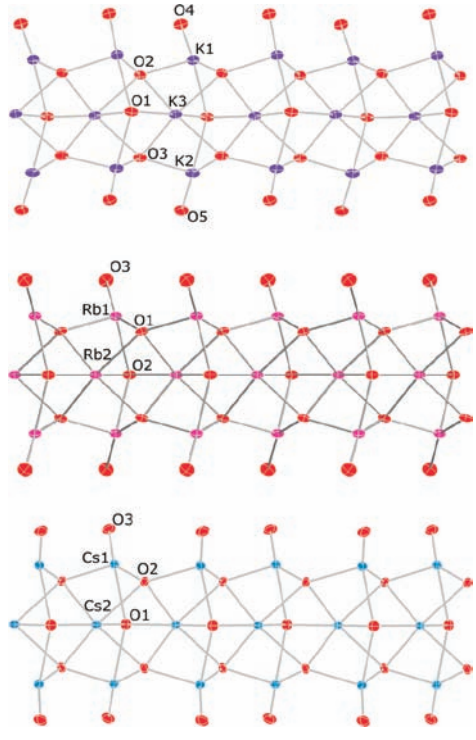

Figure 3. Thermal ellipsoid plots of (top) **3**, (middle) **4**, and (bottom) **5**. All carbon and hydrogen atoms have been removed for clarity.

dx.doi.org/10.1021/ic202158m | *Inorg. Chem.* 2012, 51, 1020−1027

cavities are efficiently filled by the 4-Et-$C_6H_4O^-$ groups, leaving essentially no solvent-accessible void space.[23] This is why it can support the 3D architecture, whereas in **1**, the space would be insufficiently filled and that leads to the 2D-layered structure.[22]

The materials **3**−**5** are isostructural and are constructed from 1D inorganic rods built from M−O_{Ar} interactions. The inorganic rods that build **3**−**5** contain two unique metal environments (Figure 3). The first is a metal center that is coordinated by six μ_4-oxygen atoms of aryloxide ligands in a very distorted octahedral geometry. The metal centers in this environment run down the center of the rods. The second environment is a metal center coordinated to three μ_4-oxygen atoms of aryloxide ligands and one oxygen atom of a bridging 1,4-dioxane. The geometry around this metal center is distorted trigonal pyramidal, in which the base is formed by the three O_{Ar} ligands and 1,4-dioxane is the apical ligand. The metal centers in this environment run along the edges of the rods. The rods are isostructural, and as expected, the metrical parameters vary only because of the size of the metal cation. A clear expansion of the rods can be observed as a measure of the M−O_{Ar} bond distances as the ionic radius of the metal increases from **3** to **4** to **5**. This trend is illustrated in Table 3 with a list of selected bond lengths for **3**−**5**. Table 4 compares **3**−**5** with other alkali-metal aryloxide inorganic rods in the literature.

Each rod is connected to four other rods by bridging 1,4-dioxanes to form parallel layers with a (4,4) net topology. Thus, the extended structure can be described as a **pcu**-type rod packing (Figure 4). The channels formed between the rods are occupied by the ethyl groups of the 4-Et-$C_6H_4O^-$ ligands, which essentially completely fill the void space. This efficient filling of the void space along with the rigidity of the inorganic rods provides the stability for the 3D architecture in **3**−**5**.

Given that the anions and solvent/linkers are identical in **1**−**5**, the explanation as to why **3**−**5** form inorganic rods must be related to the cation size. Specifically, the steric bulk in close proximity to the metal center is the most important factor. Going down group 1, as the ionic radius increases, so does the maximum coordination number of the metal center.[54] In **1**, the lithium metal centers are all four-coordinate. In **2**, the two central sodium metals are five-coordinate. When the ionic radius of the metal reaches beyond that of sodium, the metals can accommodate up to six ligands, as is seen with the central metals in **3**−**5**. It seems 6 is the maximum coordination number in this system.

The characterization of **3**−**5** opens the opportunity to review whether any structural patterns are emerging for alkali-metal rod architectures. Figure 5 shows a portion of each alkali-metal inorganic rod, excluding simple chain[12] and ladder[55] structures, reported to date. The connectivity of the previously reported alkali-metal aryloxide rods vary from simple face-sharing cubanes with just one edge missing, [(2-Me-$C_6H_4OK)_2$·(THF)],[12] (Figure 5f), to the quite complex helical rods in [(4-Br-$C_6H_4ORb)_5$·$(dioxane)_5$][10] (Figure 5g). Interestingly, the rods in $(C_6H_5OM)_3$ (M = K, Rb, Cs), [(4-Cl-$C_6H_4OK)_3$·dioxane], and [(4-Br-$C_6H_4OK)_2$·$(dioxane)_{0.5}$] (Figure 5a−e) have connectivity virtually identical with that of compounds **3**−**5**.[10,13] The simple phenoxide rods are solvent-free and thus are not decorated with 1,4-dioxane molecules as in **3**−**5**, [(4-Cl-$C_6H_4OK)_3$·dioxane] and [(4-Br-$C_6H_4OK)_2$·$(dioxane)_{0.5}$]. These solvent-free rods adopt a hexagonal packing array. [(4-Cl-$C_6H_4OK)_3$·dioxane] and [(4-Br-$C_6H_4OK)_2$·$(dioxane)_{0.5}$] form **pcu** extended structures similar to those of compounds **3**−**5**. This similarity is most likely attributable to the similarity in local steric bulk at the metal centers. Because varying the para substituent on an aryloxide does not affect the coordination number of the metal, it does not influence the aggregation state. On the other hand, [(2-Me-$C_6H_4OK)_2$(THF)] is substituted at the ortho position, and that likely is one reason that the inorganic rod formed is different from those of **3**−**5**. The helical rods in [(4-Br-$C_6H_4ORb)_5$·$(dioxane)_5$] do not connect together to form an extended network. The coordinating 1,4-dioxane molecules do not bridge, leaving the parallel rods to pack in a hexagonal packing array.[10] The other rods in Figure 5i−k are not built from aryloxide anions, and so they should not be expected to form rods similar to those of **3**−**5**. However,

Table 3. Selected Bond Distances (Å) for Compounds 3−5

3		4		5	
K1−O1	2.691(6)	Rb1−O1	2.923(4)	Cs1−O1	2.9746(17)
K1−O2	2.790(6)	Rb1−O1a	2.856(4)	Cs1−O2	3.015(5)
K1−O2a	2.823(5)	Rb1−O2	2.8066(18)	Cs1−O2a	3.139(5)
K2−O1	2.682(6)	Rb2−O1	2.811(4)	Cs2−O1	2.962(7)
K2−O3	2.747(6)	Rb2−O1a	2.943(4)	Cs2−O1a	3.172(7)
K2−O3a	2.784(5)	Rb2−O1b	2.811(4)	Cs2−O2	2.967(5)
K3−O1	2.714(3)	Rb2−O1c	2.943(4)	Cs2−O2a	3.120(5)
K3−O1a	2.969(3)	Rb2−O2	2.809(6)	Cs2−O2b	2.967(5)
K3−O2	2.647(5)	Rb2−O2a	3.067(6)	Cs2−O2c	3.120(5)
K3−O2a	2.814(6)				
K3−O3	2.672(6)				
K3−O3a	2.831(6)				

Table 4. Average M−O_{Ar} Distances in Alkali-Metal Aryloxide Inorganic Rods

	av M1−O_{Ar} (Å)	av M2−O_{Ar} (Å)	av M3−O_{Ar} (Å)	av M4−O_{Ar} (Å)	av M5−O_{Ar} (Å)	ref
(C_6H_5ONa)	2.33					13
$(C_6H_5OK)_3$	2.82	2.73	2.74			13
[(4-Et-$C_6H_4OK)_3$·dioxane]	2.77	2.73	2.77			[a]
[(2-Me-$C_6H_4OK)_2$(THF)]	2.74	2.76				12
[(4−Cl-$C_6H_4OK)_3$·dioxane]	2.73	2.74	2.75			10
[(4−Br-$C_6H_4OK)_2$·$(dioxane)_{0.5}$]	2.75	2.75				10
$(C_6H_5ORb)_3$	2.97	2.87	2.89			13
[(4-Et-$C_6H_4ORb)_2$·$(dioxane)_{0.5}$]	2.86	2.89				[a]
[(4−Br-$C_6H_4ORb)_5$ ·$(dioxane)_5$]	2.87	2.93	2.89	2.88	2.90	10
$(C_6H_5OCs)_3$	3.09	3.04	3.09			13
[(4-Et-$C_6H_4OCs)_2$·$(dioxane)_{0.5}$]	3.04	3.05				[a]

[a]This work.

dx.doi.org/10.1021/ic202158m | Inorg. Chem. 2012, 51, 1020−1027

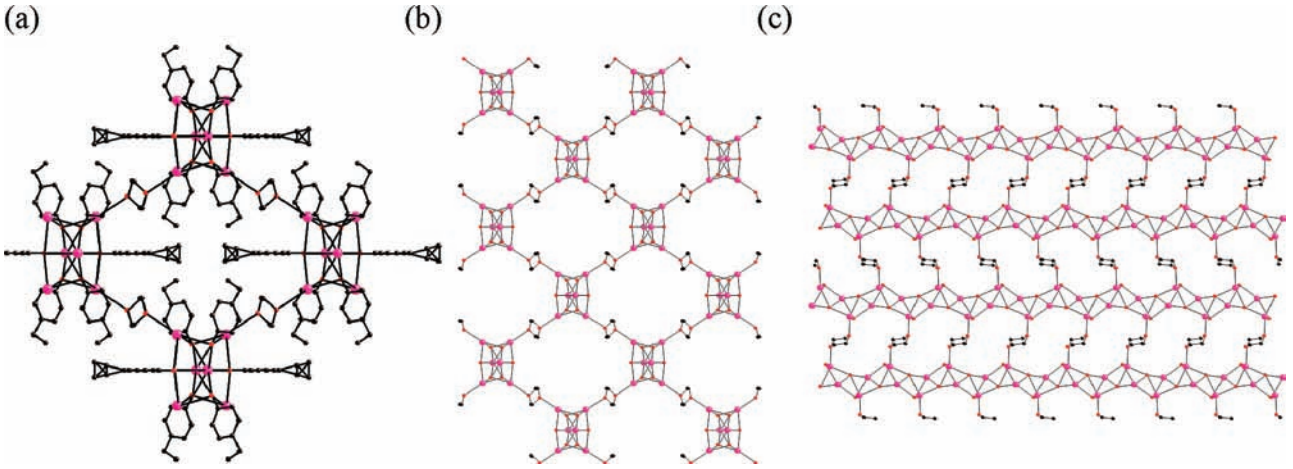

Figure 4. (a) Portion of **4** showing one channel, (b) a wider view with all aryloxide carbon atoms removed, and (c) a side view of the structure showing the inorganic rods with all aryloxide carbon atoms removed for clarity. All hydrogen atoms are removed for clarity.

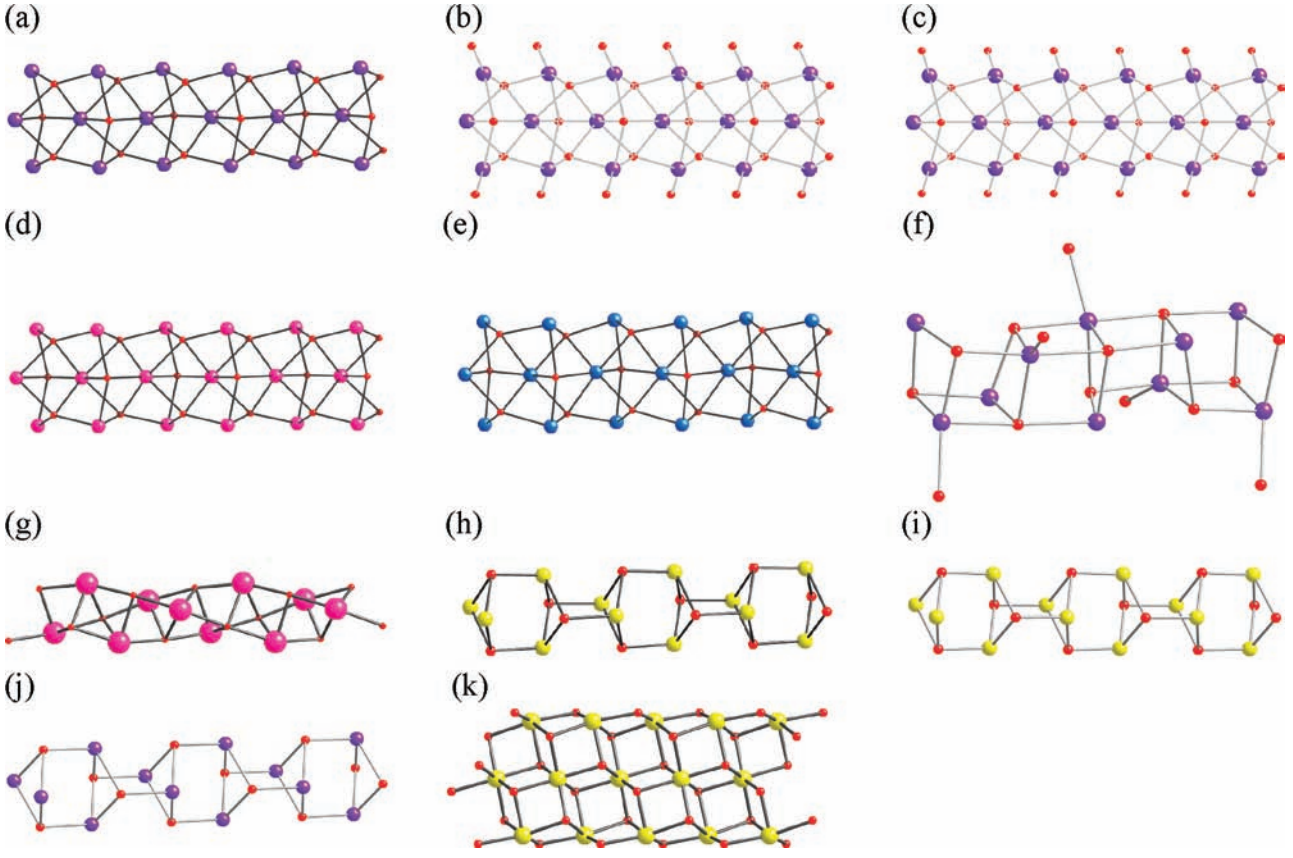

Figure 5. Sections of the inorganic rods of (a) $(C_6H_5OK)_3$,[13] (b) $[(4\text{-Cl-}C_6H_4OK)_3\cdot diox]$,[10] (c) $[(4\text{-Br-}C_6H_4OK)_2\cdot(diox)_{0.5}]$,[10] (d) $(C_6H_5ORb)_3$,[13] (e) $(C_6H_5OCs)_3$,[13] (f) $[(2\text{-Me-}C_6H_4OK)_2(THF)]$,[12] (g) $[(4\text{-Br-}C_6H_4ORb)_5\cdot(diox)_5]$,[10] (h) (C_6H_5ONa),[13] (i) $Na_2(p\text{-}C_6H_4O_2)$,[56] (j) $K_2(p\text{-}C_6H_4O_2)$,[57] and (k) $Na_2(C_5H_4NCO_2)_2$.[58] Color code: Na, yellow; K, purple; Rb, pink; Cs, blue; O, red.

the (C_6H_5ONa) rod[13] is isostructural to the $[M_2(p\text{-}C_6H_4O_2)]$ (M = Na, K) rods.[56,57]

While the extended structures of **3**–**5** are topologically the same, the coordination angles of the bridging 1,4-dioxane molecules are quite different. Through measurement of the angle $O'_{diox}\text{–}O_{diox}\text{–}M$, it is clear that, as the size of the metal cation changes, the coordination angle of the 1,4-dioxane bridge is quite flexible. There are two crystallographically independent K/diox environments in **3**, which have coordination angles of O4′–O4–K1 = 157.0° and O5′–O5–K2 = 164.1°, and only one in each of **4** (O3′–O3–Rb1 = 155.2°) and **5** (O3′–O3–Cs1 = 121.7°). The difference between K2 and Cs1 is greater than 42°, as shown in Figure 6. It should also be noted that between all structures the metrical parameters within the 1,4-dioxane molecules remain very similar. Rather, it is the flexibility in the coordination environment of 1,4-dioxane to the metal centers that accounts for the large differences in the bridging angles.

dx.doi.org/10.1021/ic202158m | *Inorg. Chem.* 2012, 51, 1020–1027

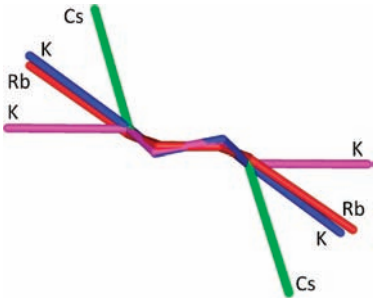

Figure 6. Overlay of bridging dioxanes in **3** (blue K1 and pink K2), **4** (red), and **5** (green) showing the differences in the coordination angles. The oxygen atoms of the dioxanes are matched up and shown bridging two metal centers.

CONCLUSIONS

This work represents just the second complete homologous series of alkali-metal aryloxides to be structurally characterized and includes the first 3D material built from cesium inorganic rods. Varying the cation size, even in the presence of identical anions and solvents, can drastically affect the solid-state structures of the resulting coordination polymers. The lithium and sodium complexes **1** and **2** form discrete aggregates that act as SBUs in the construction of 2D and 3D extended structures, respectively. The heavier alkali-metal analogues, **3**–**5**, form isostructural 1D inorganic rods that then connect to form hybrid organic–inorganic materials. The observation that the aggregation state increases as heavier alkali metals are used is due to the increased ionic radii of the cations. The larger ionic radii allow a greater coordination number, which leads to larger aggregates in this series. In the case of potassium, rubidium, and cesium, an increase in the coordination number leads to the formation of 1D rods. This allows the larger alkali metals to fill their coordination spheres with the anionic O_{Ar} as opposed to the neutral O_{diox} interactions. Even though the inorganic rod building units are isostructural, the increasing cation size in **3**–**5** is reflected in varying coordination angles of the bridging 1,4-dioxane molecules.

The inorganic rods that build **3**–**5** are virtually identical with the two potassium rods previously described in the literature and the heavier homologues of the alkali-metal phenoxide system.[10,13] Thus, a pattern does seem to be emerging from this limited set that suggests that the construction of these rods is inherently favorable. However, a larger sample size of characterized complexes is required before drawing conclusions. We are currently exploring other anion/solvent systems to determine if this pattern of large metals forming inorganic rods is a general trend for alkali-metal aryloxides or if it is specific to a few anion/solvent systems.

ASSOCIATED CONTENT

Supporting Information

Crystallographic data for compounds **3**–**5** in CIF format. This material is available free of charge via the Internet at http://pubs.acs.org.

AUTHOR INFORMATION

Corresponding Author

*E-mail: khenders@nd.edu. Phone: 574-631-8025. Fax: 574-631-6652.

ACKNOWLEDGMENTS

We gratefully acknowledge support of the Bayer Corp. and the Center for Sustainable Energy at Notre Dame (cSEND).

REFERENCES

(1) Czaja, A. U.; Trukhan, N.; Müller, U. *Chem. Soc. Rev.* **2009**, *38*, 1284–1293.
(2) Férey, G. *Chem. Soc. Rev.* **2008**, *37*, 191–214.
(3) Horike, S.; Shimomura, S.; Kitagawa, S. *Nat. Chem.* **2009**, *1*, 695–704.
(4) Perry, J. J.; Perman, J. A.; Zaworotko, M. J. *Chem. Soc. Rev.* **2009**, *38*, 1400–1417.
(5) Tranchemontagne, D. J.; Mendoza-Cortés, J. L.; O'Keeffe, M.; Yaghi, O. M. *Chem. Soc. Rev.* **2009**, *38*, 1257–1283.
(6) Ockwig, N. W.; Delgado-Friedrichs, O.; O'Keeffe, M.; Yaghi, O. M. *Acc. Chem. Res.* **2005**, *38*, 176–182.
(7) Cheetham, A. K.; Rao, C. N.; Feller, R. K. *Chem. Commun.* **2006**, 4780–4795.
(8) Feller, R. K.; Cheetham, A. K. *Solid State Sci.* **2006**, *8*, 1121–1125.
(9) Guillou, N.; Livage, C.; van Beek, W.; Nogues, M.; Ferey, G. *Angew. Chem., Int. Ed.* **2003**, *42*, 643–647.
(10) Morris, J. J.; Noll, B. C.; Henderson, K. W. *Inorg. Chem.* **2008**, *47*, 9583–9591.
(11) Rosi, N. L.; Kim, J.; Eddaoudi, M.; Chen, B.; O'Keeffe, M.; Yaghi, O. M. *J. Am. Chem. Soc.* **2005**, *127*, 1504–1518.
(12) Boyle, T. J.; Andrews, N. L.; Rodriguez, M. A.; Campana, C.; Yiu, T. *Inorg. Chem.* **2003**, *42*, 5357–5366.
(13) Dinnebier, R. E.; Pink, M.; Sieler, J.; Stephens, P. W. *Inorg. Chem.* **1997**, *36*, 3398–3401.
(14) Schade, C.; Schleyer, P. v. R. *Adv. Organomet. Chem.* **1987**, *27*, 169–278.
(15) Boche, G. *Angew. Chem., Int. Ed.* **1989**, *28*, 277–297.
(16) Gregory, K.; Schleyer, P. v. R.; Snaith, R. *Adv. Inorg. Chem.* **1991**, *37*, 47–142.
(17) Fromm, K. M.; Gueneau, E. D. *Polyhedron* **2004**, *23*, 1479–1504.
(18) Mulvey, R. E. *Acc. Chem. Res.* **2009**, *42*, 743–755.
(19) Henderson, K. W.; Kennedy, A. R.; McKeown, A. E.; Strachan, D. *J. Chem. Soc., Dalton Trans.* **2000**, 4348–4353.
(20) Henderson, K. W.; Kennedy, A. R.; MacDougall, D. J.; Shanks, D. *Organometallics* **2002**, *21*, 606–616.
(21) Henderson, K. W.; Kennedy, A. R.; Macdonald, L.; MacDougall, D. J. *Inorg. Chem.* **2003**, *42*, 2839–2841.
(22) MacDougall, D. J.; Morris, J. J.; Noll, B. C.; Henderson, K. W. *Chem. Commun.* **2005**, 456–458.
(23) MacDougall, D. J.; Noll, B. C.; Henderson, K. W. *Inorg. Chem.* **2005**, *44*, 1181–1183.
(24) MacDougall, D. J.; Noll, B. C.; Kennedy, A. R.; Henderson, K. W. *Dalton Trans.* **2006**, 1875–1884.
(25) Morris, J. J.; Noll, B. C.; Henderson, K. W. *Cryst. Growth Des.* **2006**, *6*, 1071–1073.
(26) Morris, J. J.; MacDougall, D. J.; Noll, B. C.; Henderson, K. W. *Dalton Trans.* **2008**, 3429–3437.
(27) Morris, J. J.; Noll, B. C.; Henderson, K. W. *Chem. Commun.* **2007**, 5191–5193.
(28) Morris, J. J.; Noll, B. C.; Honeyman, G. W.; O'Hara, C. T.; Kennedy, A. R.; Mulvey, R. E.; Henderson, K. W. *Chem.—Eur. J.* **2007**, *13*, 4418–4432.
(29) Morris, J. J.; Noll, B. C.; Schultz, A. J.; Piccoli, P. M.; Henderson, K. W. *Inorg. Chem.* **2007**, *46*, 10473–10475.
(30) Li, D.; Wang, S.; Xu, H.; Yang, Y.; Zeng, S.; Zhao, J.; Wang, D.; Dou, J. *Inorg. Chim. Acta* **2011**, 85–95.
(31) Long, D. L.; Blake, A. J.; Champness, N. R.; Wilson, C.; Schroder, M. *Angew. Chem., Int. Ed.* **2001**, *40*, 2443–2447.
(32) Ren, P.; Shi, W.; Cheng, P. *Inorg. Chem. Commun.* **2008**, *11*, 125–128.

(33) Zhang, Y. B.; Zhang, W. X.; Feng, F. Y.; Zhang, J. P.; Chen, X. M. *Angew. Chem., Int. Ed.* **2009**, *48*, 5287−5290.
(34) Zhang, Z.; Xiang, S.; Zheng, Q.; Rao, X.; Mondal, J. U.; Arman, H. D.; Qian, G.; Chen, B. *Cryst. Growth Des.* **2010**, *10*, 2372−2375.
(35) Kim, E. J.; Kim, C. H.; Yun, S. S. *Acta Crystallogr., Sect. C: Cryst. Struct. Commun.* **2007**, *63*, m427−m429.
(36) Chaloner, P. A.; Hitchcock, P. B.; Sutton, P. G. *J. Chem. Res.* **1998**, 186−186.
(37) Prondzinski, N. V.; Winter, M.; Merz, K. *Acta Crystallogr., Sect. E: Struct. Rep. Online* **2007**, *63*, m1687−m1687.
(38) Yang, Z.; Hu, M.; Wang, X. *Acta Crystallogr., Sect. E: Struct. Rep. Online* **2007**, *64*, m225−m225.
(39) Hu, M.; Geng, C.; Li, S.; Du, Y.; Jiang, Y.; Liu, Z. *J. Organomet. Chem.* **2005**, *690*, 3118−3124.
(40) Harrowfield, J. M.; Skelton, B. W.; White, A. H. *Aust. J. Chem.* **1995**, *48*, 1311−1331.
(41) Mootz, D.; Zinnius, A.; Bottcher, B. *Angew. Chem., Int. Ed.* **1969**, *8*, 378−379.
(42) Driess, M.; Pritzkow, H.; Skipinski, M.; Winkler, U. *Organometallics* **1997**, *16*, 5108−5112.
(43) Williard, P. G. *Acta Crystallogr., Sect. C: Cryst. Struct. Commun.* **1988**, *44*, 270−272.
(44) Neander, S.; Behrens, U. *Z. Anorg. Allg. Chem.* **1999**, *625*, 1429−1434.
(45) Nekola, H.; Olbrich, F.; Behrens, U. *Z. Anorg. Allg. Chem.* **2002**, *628*, 2067−2070.
(46) Chisholm, M. H.; Drake, S. R.; Naiini, A. A.; Streib, W. E. *Polyhedron* **1991**, *10*, 337−345.
(47) Nichols, M. A.; Williard, P. G. *J. Am. Chem. Soc.* **1993**, *115*, 1568−1572.
(48) Walfort, B.; Lameyer, L.; Weiss, W.; Herbst-irmer, R.; Bertermann, R.; Rocha, J.; Stalke, D. *Chem.—Eur. J.* **2001**, *7*, 1417−1423.
(49) Kunert, M.; Dinjus, E.; Nauck, M.; Sieler, J. *Chem. Ber.* **1997**, *130*, 1461−1465.
(50) Knizek, J.; Krossing, I.; Noth, H.; Schwenk, H.; Seifert, T. *Chem. Ber.* **1997**, *130*, 1053−1062.
(51) Kückmann, T. I.; Bolte, M.; Wagner, M.; Lerner, H. *Z. Anorg. Allg. Chem.* **2007**, *633*, 290−297.
(52) Balloch, L.; Drummond, A. M.; García-Alvarez, P.; Graham, D. V.; Kennedy, A. R.; Klett, J.; Mulvey, R. E.; O'Hara, C. T.; Rodger, P. J.; Rushworth, I. D. *Inorg. Chem.* **2009**, *48*, 6934−6944.
(53) Englich, U.; Chadwick, S.; Ruhlandt-Senge, K. *Inorg. Chem.* **1998**, *37*, 283−293.
(54) Clegg, W.; Russo, L. *Cryst. Growth Des.* **2009**, *9*, 1158−1163.
(55) Weinert, C. S.; Fanwick, P. E.; Rothwell, I. P. *Inorg. Chem.* **2003**, *42*, 6089−6094.
(56) Couhorn, U.; Dronskowski, R. *Z. Anorg. Allg. Chem.* **2003**, *629*, 2554−2558.
(57) Couhorn, U.; Dronskowski, R. *Z. Anorg. Allg. Chem.* **2004**, *630*, 427−433.
(58) Forsyth, C. M.; Dean, P. M.; MacFarlane, D. R. *Acta Crystallogr., Sect. C: Cryst. Struct. Commun.* **2007**, *63*, m169−m170.